REVIEW

Conformational plasticity of the Ebola virus matrix protein

Jens Radzimanowski,[1,2] Gregory Effantin,[1,2] and Winfried Weissenhorn[1,2]*

[1]University Grenoble Alpes, UVHCI, F-38000 Grenoble, France
[2]CNRS, UVHCI, F-38000 Grenoble, France

Received 9 July 2014; Revised 1 August 2014; Accepted 4 August 2014
DOI: 10.1002/pro.2541
Published online 26 August 2014 proteinscience.org

Abstract: Filoviruses are the causative agents of a severe and often fatal hemorrhagic fever with repeated outbreaks in Africa. They are negative sense single stranded enveloped viruses that can cross species barriers from its natural host bats to primates including humans. The small size of the genome poses limits to viral adaption, which may be partially overcome by conformational plasticity. Here we review the different conformational states of the Ebola virus (EBOV) matrix protein VP40 that range from monomers, to dimers, hexamers, and RNA-bound octamers. This conformational plasticity that is required for the viral life cycle poses a unique opportunity for development of VP40 specific drugs. Furthermore, we compare the structure to homologous matrix protein structures from Paramyxoviruses and Bornaviruses and we predict that they do not only share the fold but also the conformational flexibility of EBOV VP40.

Keywords: Ebola virus; VP40; budding; assembly

Introduction

Ebola virus (EBOV) and Marburg virus constitute the two genera of the family Filoviridae. Marburg virus is represented by a single species and EBOV by five species.[1] The natural reservoirs of filoviruses are a number of different bat species and human transmission is thought to occur via animal hosts including primates.[1] In humans EBOV infections cause a severe hemorrhagic fever, which is mostly lethal.[2] Filoviruses are membrane enveloped filamentous viruses that contain a negative sense single stranded RNA genome grouping them together with the *Paramyxoviridae*, *Rhabdoviridae,* and *Bornaviridae* to the order Mononegavirales. Their genome encodes five nucleocapsid-associated proteins, the nucleoprotein NP, VP35, VP30, VP24, and the RNA-dependent RNA polymerase L, in addition to the matrix protein VP40 and the glycoprotein GP. Cryo electron microscopy reconstruction of the nucleocapsid core composed of NP, VP35, and VP24 revealed helical structures containing the viral genome,[3,4] which are structurally similar to other negative strand RNA virus nucleocapsids.[5–7] The helical nucleocapsid complex associates with VP30,[8] which is structurally similar to M2-1 of paramyxoviruses and may thus have a similar function as transcription antiterminator.[9–11] Finally the polymerase L completes the nucleocapsid complex and transcription and replication are likely to resemble those of other negative strand RNA viruses.[12] VP35 physically links the nucleocapsid complex to the matrix protein VP40[13,14] which is the most abundant viral protein that polymerizes underneath the viral membrane.[15] VP40 plays an essential role in virus budding and expression of VP40 is sufficient to form filamentous virus-like particles (VLP).[16,17] VP40 also

*Correspondence to: Winfried Weissenhorn, UVHCI c/o CIBB, 71 Avenue des Martyrs, 38042 Grenoble, France.
E-mail: weissenhorn@embl.fr

recruits the nucleocapsid and the glycoprotein GP to the plasma membrane for assembly and budding.[18–20] The glycoprotein GP mediates entry into target cells via the endo-lysosomal pathway,[21,22] which is mediated by extensive conformational rearrangements of GP.[23,24]

Transport of Viral Proteins

In order to orchestrate assembly all components need to concentrate at the budding site. Nucleocapsids are assembled within perinuclear inclusions, which are sites of virus replication.[25] Marburg virus nucleocapsids are transported along actin filaments and once they reach the plasma membrane the nucleocapsid associates with VP40 and is transferred to filopodia,[26] which constitute the preferred site of Marburg virus budding.[27] GP reaches the plasma membrane via the secretory pathway and concentrates at sites of VP40 accumulation.[28] Marburg virus VP40 is recruited to the plasma membrane via the retrograde endosomal transport[29] and EBOV VP40 was shown to move along actin filaments.[30] Consistent with the above data, imaging of EBOV replication demonstrated that NP, VP35, VP30, VP24, and VP40 accumulate in cytoplasmic inclusions, which enlarge near the nucleus and are subsequently transferred to the plasma membrane.[31] Budding of Marburg virus occurs via a lateral interaction of the nucleocapsid with the plasma membrane in concert with VP40 and GP. Membrane wrapping then starts at one end of the nucleocapsid and proceeds to a final envelopment and virus release via membrane scission.[32]

VP40 Recruits the ESCRT Machinery

Final steps in budding depend on endosomal sorting complexes required for transport (ESCRTs), which are recruited to viral budding sites via late domains present in viral structural proteins.[33–36] EBOV VP40 contains two overlapping late domains and Marburg virus has the same motifs present in VP40 and NP.[37–39] EBOV VP40 interacts with Tsg101 via its PTAP motif *in vivo*[40] consistent with the presence of Tsg101 in VP40 containing VLPs.[41] The second late domain was first shown to bind to a WW domain from the yeast E3 ligase Rsp5 (Nedd4 homologue)[42] and later to the WW domain 3 from human Nedd4 *in vitro*.[43] Notably dominant negative mutants of Nedd4 inhibit budding of VP40 containing VLPs[44] and dominant negative VPS4 inhibits Marburg virus release.[45] This is consistent with the current model that stipulates that late domains present in viral structural proteins serve to provide access to ESCRT-III and the VPS4 complex, which constitute the membrane fission machinery. ESCRT-III is thought to assemble into filamentous helical structures within the neck of a budding virion, constrict the membrane neck via the formation of dome-like structures[46,47] and induce scission in concert with the VPS4 ATPase.[36,48] However, other factors may be able to substitute for ESCRTs during filovirus budding, because late domain mutations do not completely inhibit budding.[45,49]

Different Conformations of the Matrix Protein VP40

The matrix protein VP40 is the major structural protein[15] and its expression in eukaryotic cells suffices to release virus-like particles (VLPs) with filamentous morphology. However, VP40 VLPs have variable diameters from 40 to 80 nm, compared to the more or less consistent 80 nm diameter of infectious virus.[16–18,42,50–53] The crystal structure of VP40 revealed two structurally related N- and C-terminal beta sandwich domains (NTD and CTD), which pack against each other in a closed conformation[54] [Fig. 1(A)]. The structure lacks the first 40 amino acids (30 residues had been removed for crystallization purposes). However this N-terminal region contributes to the stability of VP40; it might reach over to the CTD because its presence increases the protease resistance of the CTD and protects it from trypsin cleavage at position 212 *in vitro*.[55] Removal of the complete CTD, the last seven residues of CTD and artificial destabilization of the NTD–CTD interface by urea leads to spontaneous oligomerization via the NTD demonstrating the metastable interaction between NTD and CTD.[55,56] The oligomeric states observed *in vitro* are hexameric and octameric ring-like structures with dimeric NTD as the building block.[55–57] The CTD, which must be linked flexibly to the NTD in these oligomers, has been implicated in membrane association.[55,56] There are two regions on the CTD which have been suggested to be important for membrane interaction. One is part of a basic patch present on the disordered CTD loop connecting α helix 7 and β strand 11 [Fig. 1(B), patch 2].Deletion of this loop or mutations within this region (K274E, K275E) inhibited VLP release from cells.[58] In contrast, another study implicated a CTD hydrophobic surface composed of residues Leu213, Ile293, Leu295, and Val298 at the opposite site of the CTD [Fig. 1(B), patch 1] as being critical for plasma membrane localization, VP40 oligomerization, and viral particle egress.[59] The same region was shown to penetrate into the plasma membrane and was shown to be important for liposome tubulation and for VP40-induced vesicle budding from giant unilamelar vesicles.[60] Furthermore mutagenesis within this region affected the intracellular localization of VP40 and caused a reduction or a complete block of VLP release.[61] Due to the distant locations of patches 1 and 2 it is unlikely that both regions are directly implicated in membrane interaction. Therefore the exact orientation of VP40 CTD on membranes needs further investigation.

This figure also includes an iMolecules 3D interactive version that can be accessed via the link at the bottom of this figure's caption.

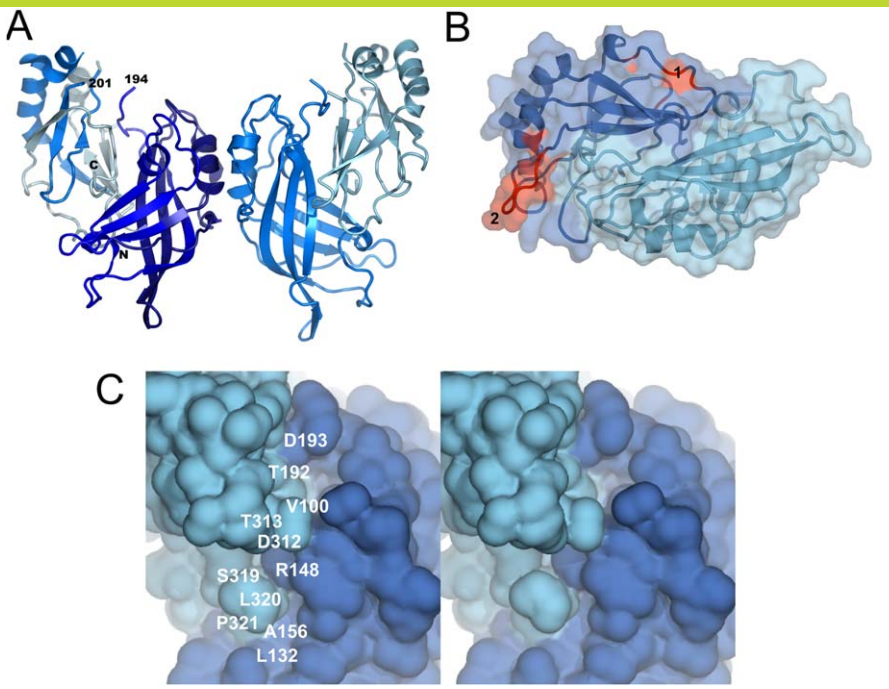

Figure 1. Crystal structure of VP40. (A) Structure of dimeric VP40 (pdb code 1ES6); The chain direction from N- to C-terminus is colored dark to light blue. Dimerization in solution has been confirmed.[58] (B) Close-up of two proposed membrane interaction motifs located at two opposing sites of the CTD. The hydrophobic surface comprising residues Leu213, Ile293, Leu295, and Val298 is indicated as patch 1 and the loop region (disordered in the crystal structure and modeled as a coil) comprising residues K274 and K275 as patch 2. Both regions shown in red have been implicated in membrane interaction. (C) The metastable association of the NTD and CTD generates two potential drug binding pockets. Stereo image of the NTD–CTD interface. Two potential drug binding pockets (residues Leu132, Ala156, Arg148, Ser319, L320, Pro321; and residues Val100, Thr192, Asp193, Asp312, and Thr313) are indicated. Binding of small molecules within these pockets could stabilize the closed conformation and thus prevent the formation of oligomeric VP40 that is required for the Ebola virus life cycle. An interactive view is available in the electronic version of the article.

VP40 has been initially shown to be monomeric in solution based on chemical cross linking experiments performed at pH 8.8 and protein concentrations of < 2 mg/mL,[55] while size exclusion chromatography and multiangle light scattering revealed dimers in solution at protein concentrations of 2 mg/mL[58] and mutagenesis of the dimer interface demonstrated its relevance for virus assembly.[58] The same authors showed that VP40 dimers assemble via CTD to CTD interactions into linear hexamers and they suggest that such hexamers form the building block for assembly. These hexamers would expose alternating CTDs towards the viral membrane and towards the nucleocapsid thus potentially establishing a firm link between the nucleocapsid and the membrane.[58] A similar arrangement exposing the CTDs alternating above and below a ring structure has been determined for hexameric VP40 ring structures assembled *in vitro*.[56] Until now no biological function has been assigned to these VP40 hexameric ring structures. Electron tomography analysis of EBOVs suggested that VP40 is arranged as a regular lattice with a 5 nm spacing, which was suggested to correspond to the hexameric assembly[3,62] [Fig. 2(A)]. In contrast other electron microscopy studies on Marburg virus revealed only local regularity within an inner and outer layer of a VP40 lattice.[14]

Dissociation of the CTD leads to an octameric ring structure that specifically binds the short RNA sequence 5′-UGA-3′. The RNA stabilizes the ring structures and confers SDS resistance to the octamer[57,63] [Fig. 3(A,B)]. Structural comparison of the NTD in complex with RNA and of the NTD associated with the CTD in the closed conformation revealed that the N-terminal 69 residues need to move out of the way to make the dimerization interface within the octamer accessible [Fig. 3(C)] Accordingly this region was disordered in the crystal structure. Furthermore the tip of β1 and β2 change conformation and interact with a neighboring molecule within the octamer [Fig. 3(A)]. No VP40 octamer formation has been observed *in vitro* in the absence of RNA.[57] This is in contrast to an RNA-free octamer crystal structure.[58] However, these crystals formed after proteolysis and therefore additional RNAse contamination could have removed the RNA; although Bornholdt et al.[58] report oligomer formation of a mutant that can no longer bind RNA, such oligomerization is likely dependent on the relatively high protein concentration used in the analysis. In

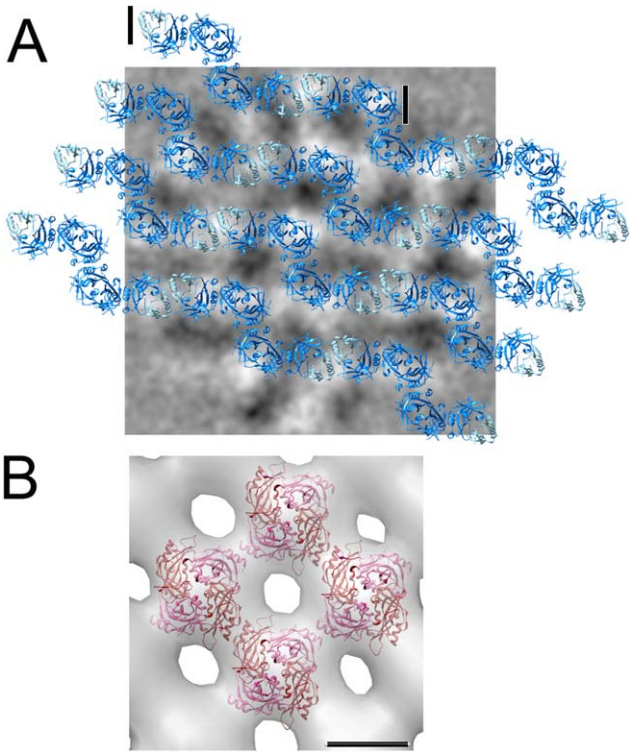

Figure 2. Structural organization of filovirus and paramyxovirus matrix proteins in virions. (A) VP40 filaments derived from the assembly of VP40 hexamers are modeled to scale onto 2D averages of virion tomograms. Black/white has been inverted for clarity in these images; white now corresponds to VP40 density. The hexamer unit as defined by the crystal structure is indicated by two black lines.[3,58] (B) Cryo electron microscopy map of the matrix protein layer of Newcastle disease virus with the matrix protein dimer docked into the density,[69] the scale bar, 5 nm.

contrast VP40 octamers have been detected upon VP40 expression in mammalian cells and in infected cells as SDS-resistant oligomers detected by western blot analysis.[53,63] Because we did not detect any octamer formation at low protein concentrations in the absence of RNA,[57] we suggest that specific RNA binding drives octamer formation under physiological conditions. In addition to the N-terminus of NTD, the CTD also has to dissociate in order to facilitate octamer formation. A flexible linker can position the CTDs at the side, above or below the ring structure. Because the CTD binds to membranes, VP40 octamers may also function at membranes. EBOV replication was shown to occur in inclusions at the perinuclear region[25,31] and the activity of VP40 octamers might be immobilized there via CTD membrane interactions. Alternatively, the CTD might associate with other viral or cellular factors required to exert its regulatory function during viral transcription.[58] The function of VP40 octamers is likely limited to transcription control because octamers are not present in virus particles[63] and VP40 mutants that no longer bind RNA can still form VLPs but do not support EBOV replication. The VP40 RNA binding activity is essential for the EBOV life cycle[53] and we hypothesize that the sequence-specific recognition of RNA is linked to the recognition of viral RNA.

Analyzing the NTD–CTD interface within the monomer reveals two pockets that could accommodate small molecules and thus stabilize the closed NTD–CTD conformation. Leu132, Ala156, and Arg148 form together with Ser319, L320, and Pro321 an $\sim 14 \times 7 \times 6.5$ Å deep pocket and Val100 and Thr192 are at the bottom of $\sim 8 \times 8 \times 10$ Å deep pocket that is surrounded by Asp193, Asp312, and Thr313 [Fig. 1(C)]. Notably removal of residues 320–326 destabilizes the NTD–CTD interaction such that the CTD dissociates, which induces spontaneous NTD oligomerization *in vitro* leading to VP40 hexamers and octamers in the presence of RNA (56). This suggests that the C-terminal end is critical for the NTD–CTD interaction. Therefore stabilizing the NTD–CTD interaction with small molecules should interfere with virus propagation notably because the generation of octameric ring-structures is essential for virus replication.[53] Hence VP40 might be a suitable drug target in order to interfere with EBOV infection.

Conservation of the VP40 Fold in Negative Strand RNA Virus Matrix Proteins

The evolutionary relationship of negative single strand RNA viruses is confirmed by the structural conservation of the matrix proteins from *Filoviridae*, *Paramyxoviridae,* and *Bornaviridae*. The exception is the matrix protein structure from Vesicular

This figure also includes an iMolecules 3D interactive version that can be accessed via the link at the bottom of this figure's caption.

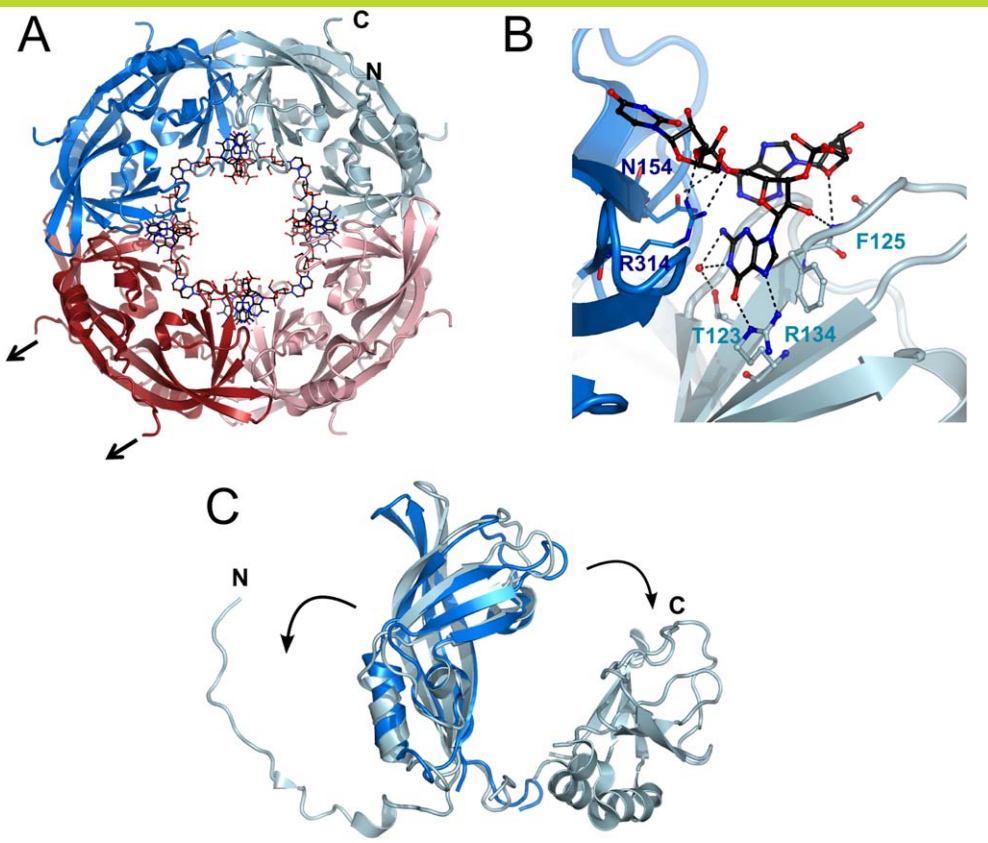

Figure 3. Octamer structure of the VP40 NTD bound the short RNA 5′-UGA-3′. (A) Full length VP40 can be destabilized to bind RNA in an octameric conformation mediated by the NTD (pdb code1H2C). An interactive view is available in the electronic version of the article.(B) Close-up of the sequence-specific RNA recognition (C) The N-terminal region of the VP40 NTD as well as the CTD need to dissociate from the core to facilitate octamer formation. The CTDs are connected by a long flexible linker allowing a more or less random positioning in solution (black arrows in A indicate their position).

stomatitis virus (VSV) a member of the Rabdoviridae. The structure of the VSV matrix protein folds into an N-terminal part composed of an anti-parallel β-sheet packed against two α-helices and a small C-terminal region[64,65] [Fig. 4(A)] with no significant structural homology to EBOV VP40. In contrast the Borna disease virus matrix protein is smaller and contains only one domain with structural homology to the NTD of VP40.[66] Borna virus matrix forms tetramers in solution and the crystal structure revealed that the tetramer binds single stranded RNA at its center which was modeled as cytidine-5′-monophosphate [Fig. 4(B)]. The functional role of the RNA bound conformation of the matrix protein is unclear. It has been detected in Borna virus infected brain tissue[67] and could thus play a role in assembly or any other step of the viral life cycle.

High structural conservation is found between EBOV VP40 and matrix proteins from *Paramyxoviridae* such as Respiratory syncytial virus matrix,[68] Newcastle disease virus matrix,[69] and human Metapneumovirus matrix.[70] They are all composed of two beta sandwich domains homologous to VP40 NTD and CTD that associate with each other. However the mode of interaction and the orientations of the CTDs with respect to the NTDs is different in all four viral matrix proteins [Fig. 4(C)]. In addition, the matrix proteins from Metapneumovirus and Newcastle disease virus were reported to form dimers in solution and in the crystal. Dimerization positions the NTD and CTD at the same side, and produces a pseudo-tetrameric arrangement, which is different from the VP40 dimers (Fig. 5), but resembles the quaternary structure of Borna disease virus matrix protein tetramers [Fig. 4(B)].[70] Its physiological relevance is indirectly supported by the fact that three different viral matrix proteins assemble into a similar quaternary structure. Human Metapneumovirus matrix also binds calcium, which is coordinated by two solvent exposed loops of the NTD. The presence of calcium was shown to substantially increase the thermostability of M.[70]

Incubation of human Metapneumovirus matrix with 1,2-dioleoyl-sn-glycero-3-phosphocholine (DOPC) produced tubular helical structures with variable diameters of ~40 nm. Helical three-dimensional reconstruction from electron microscopy images revealed a subunit arrangement with a rise of 5.16 Å. The repeating unit fits the dimeric crystal structure, when positioned with its dimeric

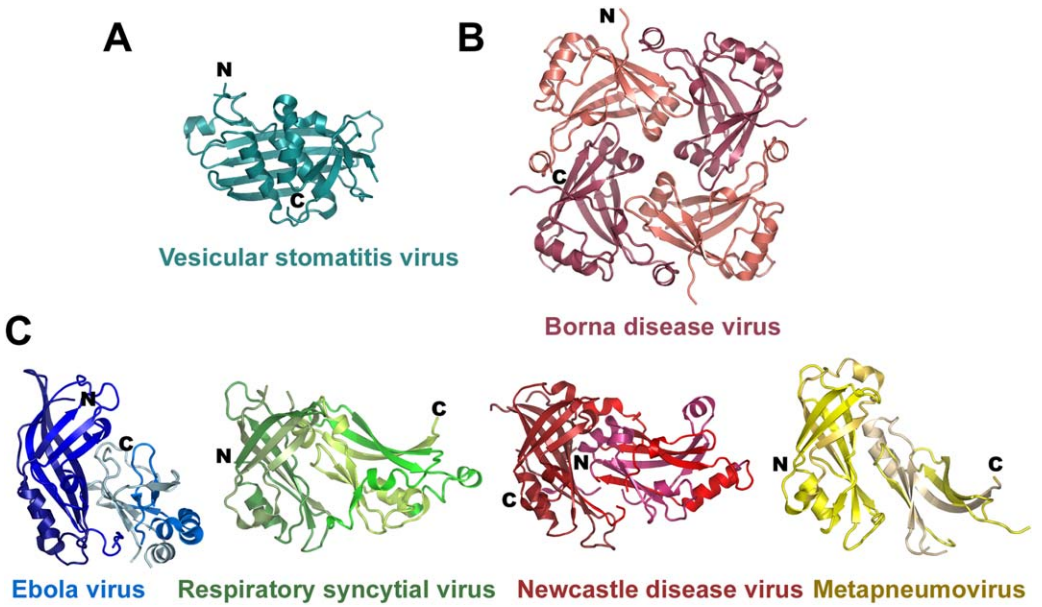

Figure 4. Structural conservation of matrix proteins from the Mononegavirales families. (A) Crystal structure of the vesicular stomatitis virus (VSV) matrix protein core (pdb code 2W2R). (B) Structure of the Borna disease virus tetramer (pdb code 3F1J). (C) Structure of the Ebola virus VP40 with the same NTD orientation as shown for RSV (pdb code 2VQP), Newcastle disease virus (pdb code 4G1L) and human Metapneumovirus (pdb code 4LP7) matrix protein monomers. (The chain direction is indicated with dark to light colors from the N- to the C-terminus.)

symmetry axis orthogonal to the long axis of the filament. This would position the concave surface of the dimer toward the inside producing a non-physiological positive curvature. Similar tubular structures of M have been observed for RSV M[71] and are found to form irregular helical assemblies in RSV virions.[72] In contrast the crystal packing of M from Metapneumovirus revealed the opposite negative curvature that is more relevant for M assembly *in vivo*.[70] In fact electron microscopy analysis of Newcastle disease virus showed an M protein layer that fits the dimeric M structure with the concave membrane binding surface positioned toward the viral membrane implicating the CTD in membrane interaction [Fig. 2(B)]. Contacts between dimers and between filaments are made by NTDs and CTDs of symmetry related units.[69] This is different from the EBOV assembly model, where NTD–NTD interactions form the filament (Fig. 2A) and the CTD contacts both the membrane and the nucleocapsid.[58]

An open question is whether the matrix proteins from Paramyxoviruses can also adopt different quaternary structures as it is the case for EBOV VP40. Money and colleagues noted that the NTD and CTD of RSV M are only kept together by weak interactions and cleavage within the linker region leads to

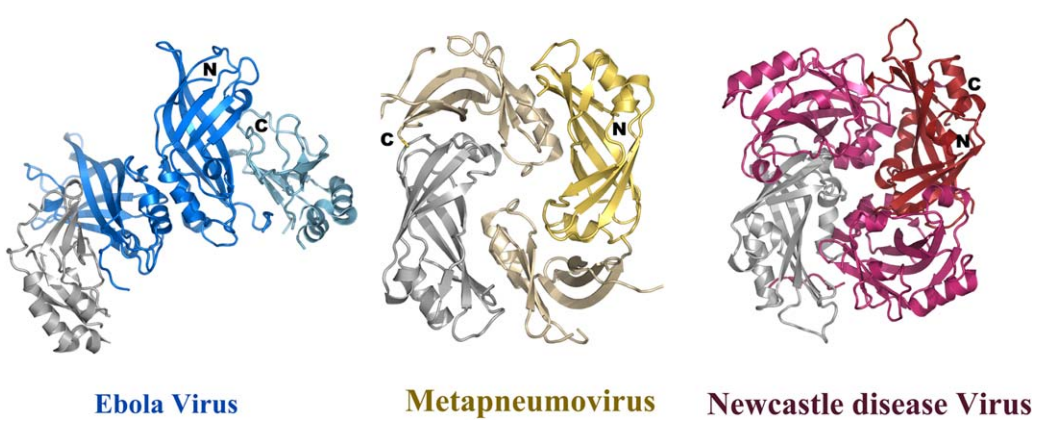

Figure 5. Comparison of dimeric structures of the matrix proteins. Dimeric conformation of the human Metapneumovirus (pdb code 4LP7) matrix protein and of Newcastle disease virus matrix (pdb code 4G1L) in comparison to the Ebola virus VP40 dimer. All three structures have one NTD (grey) in the same orientation. This demonstrates that not only the orientations of the NTD with respect to the CTD are different as shown in Figure 4, but also their mode of dimerization. It should be noted however, that the dimerization mode is quite similar for Metapneumovirus and Newcastle disease virus matrix proteins.

Table I. *Calculated Total Buried Area by the NTD–CTD Interface and Binding Energies (ΔG Indicates the Solvation Free Energy Gain upon Formation of the Assembly) for NTD–CTD Interactions of Ebola Virus VP40, Respiratory Syncytial Virus Matrix, Newcastle Disease Virus Matrix and Human Metapneumovirus Matrix using the PISA Server*[73]

	Buried area (Å^2)	ΔG (kcal/mol)
Ebola virus VP40	1365	−21.7
Respiratory syncytila virus matrix	977	−10.6
Newcastle disease virus matrix	1679	−18.4
Human Metapneumovirus matrix	760	−9.9
Gp41-HK20 Fab complex	5590	−35

For comparison the total buried surface and calculated ΔG are indicated for a high affinity antigen-antibody interaction (gp41-HK20).[74]

the dissociation of NTD and CTD.[68] Furthermore Leyrat and colleagues noted that NTD–CTD interface residues are conserved within EBOV and Metapneumovirus matrix proteins despite their overall low sequence similarity.[70] Comparison of the NTD–CTD interfaces of the known paramyxovirus matrix protein structures indicates that their interaction is relatively weak in agreement with their calculated total buried surface area that range from ∼700 to 1600 Å^2 and corresponding dissociation energies (ΔG) ranging from −21.7 to −9.9 kcal/mol, with Ebola VP40 having the highest ΔG (Table I). This suggests that these matrix protein structures can also change their NTD–CTD arrangements to produce new conformations that might play additional role(s) during the life cycle of these viruses.

Conclusions

The different conformations and quaternary structures of VP40, monomer/dimer, octamers in complex with RNA, ring-like hexamers observed *in vitro* and linear hexamers observed in the crystal are prime examples of how the small size of a viral genome can enlarge its coding capacity by packing different functions into different conformations of the same protein. Comparison of the matrix protein structures from three different families of negative single stranded RNA viruses has unraveled their evolutionary relationship that was not evident from the primary sequences highlighting once more the contribution of structural biology to the understanding of evolutionary relationships. Although the current structures have brought much insight into how these matrix proteins assemble into higher order protein networks that drive and coordinate the budding process, further work is required to determine whether the conformational plasticity observed for EBOV VP40 is also conserved in case of the matrix proteins from paramyxoviruses and Borna virus.

Acknowledgments

Work in the author's lab is supported by the CNRS, the University Joseph Fourier and the Grenoble Instruct center (ISBG; UMS 3518 CNRS-CEA-UJF-EMBL) with support from FRISBI (ANR-10-INSB-05-02) and GRAL (ANR-10-LABX-49-01). G.E. is supported by a postdoctoral fellowship from the ANRS (Agence nationale de recherché sur le sida et les hépatites virales) and J.R. by the Labex GRAL (ANR-10-LABX-49-01).

References

1. Olival KJ, Hayman DT (2014) Filoviruses in bats: current knowledge and future directions. Viruses 6:1759–1788.
2. Kuhn JH (2008) Filoviruses. A compendium of 40 years of epidemiological, clinical, and laboratory studies. Arch Virol Suppl 20:13–360.
3. Beniac DR, Melito PL, Devarennes SL, Hiebert SL, Rabb MJ, Lamboo LL, Jones SM, Booth TF (2012) The organisation of Ebola virus reveals a capacity for extensive, modular polyploidy. PloS One 7:e29608.
4. Bharat TA, Noda T, Riches JD, Kraehling V, Kolesnikova L, Becker S, Kawaoka Y, Briggs JA (2012) Structural dissection of Ebola virus and its assembly determinants using cryo-electron tomography. Proc Natl Acad Sci USA 109:4275–4280.
5. Albertini AA, Schoehn G, Weissenhorn W, Ruigrok RW (2008) Structural aspects of rabies virus replication. Cell Mol Life Sci 65:282–294.
6. Ruigrok RW, Crepin T, Kolakofsky D (2011) Nucleoproteins and nucleocapsids of negative-strand RNA viruses. Curr Opin Microbiol 14:504–510.
7. Bakker SE, Duquerroy S, Galloux M, Loney C, Conner E, Eleouet JF, Rey FA, Bhella D (2013) The respiratory syncytial virus nucleoprotein-RNA complex forms a left-handed helical nucleocapsid. J Gen Virol 94:1734–1738.
8. Hartlieb B, Muziol T, Weissenhorn W, Becker S (2007) Crystal structure of the C-terminal domain of Ebola virus VP30 reveals a role in transcription and nucleocapsid association. Proc Natl Acad Sci USA 104:624–629.
9. Blondot ML, Dubosclard V, Fix J, Lassoued S, Aumont-Nicaise M, Bontems F, Eleouet JF, Sizun C (2012) Structure and functional analysis of the RNA- and viral phosphoprotein-binding domain of respiratory syncytial virus M2-1 protein. PLoS Pathog 8:e1002734.
10. Tanner SJ, Ariza A, Richard CA, Kyle HF, Dods RL, Blondot ML, Wu W, Trincao J, Trinh CH, Hiscox JA, Carroll MW, Silman NJ, Eleouet JF, Edwards TA, Barr JN (2014) Crystal structure of the essential transcription antiterminator M2-1 protein of human respiratory syncytial virus and implications of its phosphorylation. Proc Natl Acad Sci USA 111:1580–1585.
11. Leyrat C, Renner M, Harlos K, Huiskonen JT, Grimes JM (2014) Drastic changes in conformational dynamics of the antiterminator M2-1 regulate transcription efficiency in Pneumovirinae. eLife 3:e02674.
12. Ivanov I, Yabukarski F, Ruigrok RW, Jamin M (2011) Structural insights into the rhabdovirus transcription/replication complex. Virus Res 162:126–137.

13. Johnson RF, McCarthy SE, Godlewski PJ, Harty RN (2006) Ebola virus VP35-VP40 interaction is sufficient for packaging 3E-5E minigenome RNA into virus-like particles. J Virol 80:5135–5144.
14. Bharat TA, Riches JD, Kolesnikova L, Welsch S, Krahling V, Davey N, Parsy ML, Becker S, Briggs JA (2011) Cryo-electron tomography of Marburg virus particles and their morphogenesis within infected cells. PLoS Biol 9:e1001196.
15. Geisbert TW, Jahrling PB (1995) Differentiation of filoviruses by electron microscopy. Virus Res 39:129–150.
16. Jasenosky LD, Neumann G, Lukashevich I, Kawaoka Y (2001) Ebola virus VP40-induced particle formation and association with the lipid bilayer. J Virol 75:5205–5214.
17. Timmins J, Scianimanico S, Schoehn G, Weissenhorn W (2001) Vesicular release of ebola virus matrix protein VP40. Virology 283:1–6.
18. Kolesnikova L, Berghofer B, Bamberg S, Becker S (2004) Multivesicular bodies as a platform for formation of the Marburg virus envelope. J Virol 78:12277–12287.
19. Kolesnikova L, Ryabchikova E, Shestopalov A, Becker S (2007) Basolateral budding of Marburg virus: VP40 retargets viral glycoprotein GP to the basolateral surface. J Infect Dis 196:S232–S236.
20. Mittler E, Kolesnikova L, Strecker T, Garten W, Becker S (2007) Role of the transmembrane domain of marburg virus surface protein GP in assembly of the viral envelope. J Virol 81:3942–3948.
21. Carette JE, Raaben M, Wong AC, Herbert AS, Obernosterer G, Mulherkar N, Kuehne AI, Kranzusch PJ, Griffin AM, Ruthel G, Dal Cin P, Dye JM, Whelan SP, Chandran K, Brummelkamp TR (2011) Ebola virus entry requires the cholesterol transporter Niemann-Pick C1. Nature 477:340–343.
22. Cote M, Misasi J, Ren T, Bruchez A, Lee K, Filone CM, Hensley L, Li Q, Ory D, Chandran K, Cunningham J (2011) Small molecule inhibitors reveal Niemann-Pick C1 is essential for Ebola virus infection. Nature 477: 344–348.
23. Weissenhorn W, Carfi A, Lee KH, Skehel JJ, Wiley DC (1998) Crystal structure of the Ebola virus membrane fusion subunit, GP2, from the envelope glycoprotein ectodomain. Mol Cell 2:605–616.
24. Lee JE, Fusco ML, Hessell AJ, Oswald WB, Burton DR, Saphire EO (2008) Structure of the Ebola virus glycoprotein bound to an antibody from a human survivor. Nature 454:177–182.
25. Hoenen T, Shabman RS, Groseth A, Herwig A, Weber M, Schudt G, Dolnik O, Basler CF, Becker S, Feldmann H (2012) Inclusion bodies are a site of ebolavirus replication. J Virol 86:11779–11788.
26. Schudt G, Kolesnikova L, Dolnik O, Sodeik B, Becker S (2013) Live-cell imaging of Marburg virus-infected cells uncovers actin-dependent transport of nucleocapsids over long distances. Proc Natl Acad Sci USA 110: 14402–14407.
27. Kolesnikova L, Bohil AB, Cheney RE, Becker S (2007) Budding of Marburgvirus is associated with filopodia. Cell Microbiol 9:939–951.
28. Mittler E, Kolesnikova L, Herwig A, Dolnik O, Becker S (2013) Assembly of the Marburg virus envelope. Cell Microbiol 15:270–284.
29. Kolesnikova L, Bamberg S, Berghofer B, Becker S (2004) The matrix protein of Marburg virus is transported to the plasma membrane along cellular membranes: exploiting the retrograde late endosomal pathway. J Virol 78:2382–2393.
30. Adu-Gyamfi E, Digman MA, Gratton E, Stahelin RV (2012) Single-particle tracking demonstrates that actin coordinates the movement of the Ebola virus matrix protein. Biophys J 103:L41–L43.
31. Nanbo A, Watanabe S, Halfmann P, Kawaoka Y (2013) The spatio-temporal distribution dynamics of Ebola virus proteins and RNA in infected cells. Scientific Rep 3:1206.
32. Welsch S, Kolesnikova L, Krahling V, Riches JD, Becker S, Briggs JA (2010) Electron tomography reveals the steps in filovirus budding. PLoS Pathog 6: e1000875.
33. Hartlieb B, Weissenhorn W (2006) Filovirus assembly and budding. Virology 344:64–70.
34. Usami Y, Popov S, Popova E, Inoue M, Weissenhorn W, Gottlinger HG (2009) The ESCRT pathway and HIV-1 budding. Biochem Soc Trans 37:181–184.
35. Peel S, Macheboeuf P, Martinelli N, Weissenhorn W (2011) Divergent pathways lead to ESCRT-III-catalyzed membrane fission. Trends Biochem Sci 36:199–210.
36. Sundquist WI, Krausslich HG (2012) HIV-1 assembly, budding, and maturation. Cold Spring Harb Perspect Med 2:a006924.
37. Morita E, Sundquist WI (2004) Retrovirus budding. Ann Rev Cell Devel Biol 20:395–425.
38. Schmitt AP, Lamb RA (2004) Escaping from the cell: assembly and budding of negative-strand RNA viruses. Curr Top Microbiol Immun 283:145–196.
39. Dolnik O, Kolesnikova L, Stevermann L, Becker S (2010) Tsg101 is recruited by a late domain of the nucleocapsid protein to support budding of Marburg virus-like particles. J Virol 84:7847–7856.
40. Martin-Serrano J, Zang T, Bieniasz PD (2001) HIV-1 and Ebola virus encode small peptide motifs that recruit Tsg101 to sites of particle assembly to facilitate egress. Nature Med 7:1313–1319.
41. Licata JM, Simpson-Holley M, Wright NT, Han Z, Paragas J, Harty RN (2003) Overlapping motifs (PTAP and PPEY) within the Ebola virus VP40 protein function independently as late budding domains: involvement of host proteins TSG101 and VPS-4. J Virol 77: 1812–1819.
42. Harty RN, Brown ME, Wang G, Huibregtse J, Hayes FP (2000) A PPxY motif within the VP40 protein of Ebola virus interacts physically and functionally with a ubiquitin ligase: implications for filovirus budding. Proc Natl Acad Sci USA 97:13871–13876.
43. Timmins J, Schoehn G, Ricard-Blum S, Scianimanico S, Vernet T, Ruigrok RW, Weissenhorn W (2003) Ebola virus matrix protein VP40 interaction with human cellular factors Tsg101 and Nedd4. J Mol Biol 326:493–502.
44. Yasuda J, Nakao M, Kawaoka Y, Shida H (2003) Nedd4 regulates egress of Ebola virus-like particles from host cells. J Virol 77:9987–9992.
45. Kolesnikova L, Strecker T, Morita E, Zielecki F, Mittler E, Crump C, Becker S (2009) Vacuolar protein sorting pathway contributes to the release of Marburg virus. J Virol 83:2327–2337.
46. Lata S, Schoehn G, Jain A, Pires R, Piehler J, Gottlinger HG, Weissenhorn W (2008) Helical structures of ESCRT-III are disassembled by VPS4. Science 321:1354–1357.
47. Fabrikant G, Lata S, Riches JD, Briggs JA, Weissenhorn W, Kozlov MM (2009) Computational model of membrane fission catalyzed by ESCRT-III. PLoS Comput Biol 5:e1000575.

48. Weissenhorn W, Poudevigne E, Effantin G, Bassereau P (2013) How to get out: ssRNA enveloped viruses and membrane fission. Current Opin Virol 3:159–167.
49. Neumann G, Ebihara H, Takada A, Noda T, Kobasa D, Jasenosky LD, Watanabe S, Kim JH, Feldmann H, Kawaoka Y (2005) Ebola virus VP40 late domains are not essential for viral replication in cell culture. J Virol 79:10300–10307.
50. Bavari S, Bosio CM, Wiegand E, Ruthel G, Will AB, Geisbert TW, Hevey M, Schmaljohn C, Schmaljohn A, Aman MJ (2002) Lipid raft microdomains: a gateway for compartmentalized trafficking of Ebola and Marburg viruses. J Exper Med 195:593–602.
51. Noda T, Sagara H, Suzuki E, Takada A, Kida H, Kawaoka Y (2002) Ebola virus VP40 drives the formation of virus-like filamentous particles along with GP. J Virol 76:4855–4865.
52. Swenson DL, Warfield KL, Kuehl K, Larsen T, Hevey MC, Schmaljohn A, Bavari S, Aman MJ (2004) Generation of Marburg virus-like particles by co-expression of glycoprotein and matrix protein. FEMS Immun Med Microbiol 40:27–31.
53. Hoenen T, Volchkov V, Kolesnikova L, Mittler E, Timmins J, Ottmann M, Reynard O, Becker S, Weissenhorn W (2005) VP40 octamers are essential for Ebola virus replication. J Virol 79:1898–1905.
54. Dessen A, Volchkov V, Dolnik O, Klenk HD, Weissenhorn W (2000) Crystal structure of the matrix protein VP40 from Ebola virus. EMBO J 19:4228–4236.
55. Ruigrok RW, Schoehn G, Dessen A, Forest E, Volchkov V, Dolnik O, Klenk HD, Weissenhorn W (2000) Structural characterization and membrane binding properties of the matrix protein VP40 of Ebola virus. J Mol Biol 300:103–112.
56. Scianimanico S, Schoehn G, Timmins J, Ruigrok RH, Klenk HD, Weissenhorn W (2000) Membrane association induces a conformational change in the Ebola virus matrix protein. EMBO J 19:6732–6741.
57. Timmins J, Schoehn G, Kohlhaas C, Klenk HD, Ruigrok RW, Weissenhorn W (2003) Oligomerization and polymerization of the filovirus matrix protein VP40. Virology 312:359–368.
58. Bornholdt ZA, Noda T, Abelson DM, Halfmann P, Wood MR, Kawaoka Y, Saphire EO (2013) Structural rearrangement of ebola virus VP40 begets multiple functions in the virus life cycle. Cell 154:763–774.
59. Adu-Gyamfi E, Soni SP, Xue Y, Digman MA, Gratton E, Stahelin RV (2013) The Ebola virus matrix protein penetrates into the plasma membrane: a key step in viral protein 40 (VP40) oligomerization and viral egress. J Biol Chem 288:5779–5789.
60. Soni SP, Adu-Gyamfi E, Yong SS, Jee CS, Stahelin RV (2013) The Ebola virus matrix protein deeply penetrates the plasma membrane: an important step in viral egress. Biophys J 104:1940–1949.
61. Reynard O, Nemirov K, Page A, Mateo M, Raoul H, Weissenhorn W, Volchkov VE (2011) Conserved proline-rich region of Ebola virus matrix protein VP40 is essential for plasma membrane targeting and virus-like particle release. J Infect Dis 204:S884–S891.
62. Booth TF, Rabb MJ, Beniac DR (2013) How do filovirus filaments bend without breaking? Trends Microbiol 21: 583–593.
63. Gomis-Ruth FX, Dessen A, Timmins J, Bracher A, Kolesnikowa L, Becker S, Klenk HD, Weissenhorn W (2003) The matrix protein VP40 from Ebola virus octamerizes into pore-like structures with specific RNA binding properties. Structure 11:423–433.
64. Gaudier M, Gaudin Y, Knossow M (2002) Crystal structure of vesicular stomatitis virus matrix protein. EMBO J 21:2886–2892.
65. Graham SC, Assenberg R, Delmas O, Verma A, Gholami A, Talbi C, Owens RJ, Stuart DI, Grimes JM, Bourhy H (2008) Rhabdovirus matrix protein structures reveal a novel mode of self-association. PLoS Pathog 4:e1000251.
66. Neumann P, Lieber D, Meyer S, Dautel P, Kerth A, Kraus I, Garten W, Stubbs MT (2009) Crystal structure of the Borna disease virus matrix protein (BDV-M) reveals ssRNA binding properties. Proc Natl Acad Sci USA 106:3710–3715.
67. Stoyloff R, Strecker A, Bode L, Franke P, Ludwig H, Hucho F (1997) The glycosylated matrix protein of Borna disease virus is a tetrameric membrane-bound viral component essential for infection. Eur J Biochem/ FEBS 246:252–257.
68. Money VA, McPhee HK, Mosely JA, Sanderson JM, Yeo RP (2009) Surface features of a Mononegavirales matrix protein indicate sites of membrane interaction. Proc Natl Acad Sci USA 106:4441–4446.
69. Battisti AJ, Meng G, Winkler DC, McGinnes LW, Plevka P, Steven AC, Morrison TG, Rossmann MG (2012) Structure and assembly of a paramyxovirus matrix protein. Proc Natl Acad Sci USA 109:13996–14000.
70. Leyrat C, Renner M, Harlos K, Huiskonen JT, Grimes JM (2014) Structure and self-assembly of the calcium binding matrix protein of human metapneumovirus. Structure 22:136–148.
71. McPhee HK, Carlisle JL, Beeby A, Money VA, Watson SM, Yeo RP, Sanderson JM (2011) Influence of lipids on the interfacial disposition of respiratory syncytical virus matrix protein. Langmuir 27:304–311.
72. Liljeroos L, Krzyzaniak MA, Helenius A, Butcher SJ (2013) Architecture of respiratory syncytial virus revealed by electron cryotomography. Proc Natl Acad Sci USA 110:11133–11138.
73. Krissinel E, Henrick K (2007) Inference of macromolecular assemblies from crystalline state. J Mol Biol 372: 774–797.
74. Sabin C, Corti D, Buzon V, Seaman MS, Lutje Hulsik D, Hinz A, Vanzetta F, Agatic G, Silacci C, Mainetti L, Scarlatti G, Sallusto F, Weiss R, Lanzavecchia A, Weissenhorn W (2010) Crystal structure and size-dependent neutralization properties of HK20, a human monoclonal antibody binding to the highly conserved heptad repeat 1 of gp41. PLoS Pathog 6:e1001195.